

Fluorine depth profiling by high-resolution 1D magnetic resonance imaging

T. Dikić^{a,d}, S.J.F. Erich^b, W. Ming^{a,*}, H.P. Huinink^{b,**}, P.C. Thüne^c,
R.A.T.M. van Benthem^a, G. de With^a

^a *Laboratory of Materials and Interface Chemistry, Eindhoven University of Technology, P.O. Box 513, 5600 MB Eindhoven, The Netherlands*

^b *Department of Applied Physics, Eindhoven University of Technology, P.O. Box 513, 5600 MB Eindhoven, The Netherlands*

^c *Schuit Institute of Catalysis, Eindhoven University of Technology, P.O. Box 513, 5600 MB Eindhoven, The Netherlands*

^d *Dutch Polymer Institute (DPI), P.O. Box 902, 5600 AX Eindhoven, The Netherlands*

Received 19 March 2007; received in revised form 3 May 2007; accepted 10 May 2007

Available online 18 May 2007

Abstract

High-resolution magnetic resonance imaging (MRI) has been used, for the first time, to measure fluorine concentration profiles with a high spatial resolution (5 μm) along the full film depth of fluorinated polyurethane films. The MRI fluorine profiles were consistent with the results obtained by X-ray photoelectron spectroscopy (XPS) in combination with microtoming. MRI is a nondestructive and potentially quantitative technique for probing the spatial distribution of small quantities of fluorine in coatings and multi-layered systems.

© 2007 Elsevier Ltd. All rights reserved.

Keywords: Magnetic resonance imaging; Fluorine depth profiling; X-ray photoelectron spectroscopy

1. Introduction

Films with fluorine-rich surfaces have many desirable properties such as water/oil repellency, low friction coefficient, and chemical resistance [1]. Surface segregation of fluorinated species (and also silicone compounds) has been used to obtain coatings with low surface energy and desired bulk properties [2–12]. In the case of thermosetting coatings, a fluorinated species contains a perfluoroalkyl group on one end and a reactive group on the other, which chemically binds the fluorinated tail to the polymer film upon cross-linking. The overall fluorine fraction in such coating systems is usually lower than 2 wt% [6–10,12]. During the course of our research [6–10], it has become clear that it is also important to profile the fluorine concentration along the full depth of a coating, in addition

to the (near) surface region that is usually probed, in order to design coatings with specific surface/bulk properties.

It is not an easy task and also appears challenging to determine the bulk fluorine level in fluorine-containing coatings, especially when the fluorine content is low, since most of the techniques that can be used are either not sensitive enough (such as Raman and FTIR for surface-segregated coatings) or destructive, such as X-ray photoelectron spectroscopy (XPS), dynamic secondary ion mass spectrometry (DSIMS) [13–16]. Full-depth profiling has been shown by using sputtering XPS [15] and DSIMS [16], but these destructive techniques may not give a true picture of fluorine depth profile due to uncontrolled reaction/degradation during data collection. Therefore, depth profiling of the fluorine concentration along the full depth of a film or in multi-layered coatings has not been addressed so far.

Recently, nondestructive profiling of hydrogen density in coatings, with a one-dimensional (1D) spatial resolution as high as 5 μm, has become possible using magnetic resonance imaging (MRI) [17]. MRI has shown to be a useful tool in

* Corresponding author. Tel.: +31 40 2473066; fax: +31 40 2445619.

** Corresponding author.

E-mail addresses: w.ming@tue.nl (W. Ming), h.p.huinink@tue.nl (H.P. Huinink).

determining diffusion of water through a film [18,19], water evaporation [20,21], cross-linking density of coatings [22,23], and evaporation of solvent and curing during film formation [24–27]. In medical research, ^{19}F MRI has already been used to image targeted tissue with fluorinated compounds as contrast agents [28–30].

In this paper a high-resolution MRI setup was used, for the first time, to study full-depth profiles of the fluorine concentration (as low as 1 wt%) in coatings in a nondestructive manner. The results obtained by MRI were compared with depth profiles obtained by XPS measurements in combination with microtoming.

2. Experimental

2.1. Preparation of fluorinated polyurethane films

Model polyurethane (PU) coatings were based on polycaprolactone (PCL) precursors with controlled functionality, including a tri-hydroxyl-functionalized PCL (TMP-PCL, $M_n = 1850$ g/mol, PDI = 1.11) and a perfluorooctyl PCL (Rf_8 -PCL-OH, $M_n = 2520$ g/mol, PDI = 1.16), both shown in Scheme 1, which were cured with a polyisocyanate crosslinker (Desmodur N3600, Bayer). The synthesis of TMP-PCL and Rf_8 -PCL-OH was according to literature [31,32] and details will be reported elsewhere. The reaction mixture was cast from *N*-methyl-pyrrolidone (Biosolve, vacuum distilled before use) solution (30 wt% solid contents) on a thin glass plate (~ 100 μm), and cured at 120 $^\circ\text{C}$ for 20 min. The NCO/OH molar ratio was kept at 1.2 to ensure the full conversion of all OH groups. Rf_8 -PCL was added in an amount according to desired fluorine mass fraction. For the purpose of microtoming, the substrate was a glass plate glued onto a metal carrier.

2.2. Depth profiling using MRI

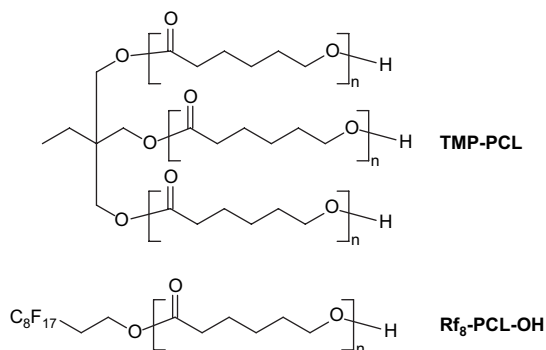
A high spatial resolution MRI setup was used for depth profiling of hydrogen and fluorine concentration in polymer films at room temperature. This relatively new technique uses the GARField design and allows profiling of coatings with a resolution of approximately 5 μm [17,24–27]. To

achieve this high spatial resolution, a high magnetic field gradient is necessary to discriminate between layers inside a coating. The home-built MRI setup consists of an electromagnet operating at 1.5 T at the sample position, and has a magnetic field gradient of 36.4 T/m perpendicular to the coating surface. For the first time this setup was used for fluorine profiling. Because of the difference in resonance frequency between hydrogen and fluorine, the magnetic field was increased by 6% to switch from hydrogen to fluorine detection. The 6% increase would prevent the fluorine and hydrogen signals from interfering with each other, since the difference in hydrogen and fluorine resonance frequency is 3.7 MHz, which is larger than the frequency difference (about 500 kHz) of the sample used in this study due to the large gradient. Switching between hydrogen and fluorine can thus be achieved without sample manipulation. As a result both fluorine and hydrogen profiles can be easily compared. The MRI profiles were corrected for inherent signal intensity variations, using profiles obtained from appropriate reference samples.

To measure fluorine profiles with a 1D spatial resolution of 5 μm in coatings with relatively low fluorine contents (1–3 wt%), the amount of averages is increased by a factor of 10^4 to obtain a similar signal-to-noise ratio as for hydrogen. The Ostroff–Waugh pulse sequence ($90^\circ_x - \tau - [90^\circ_y - \tau - \text{echo} - \tau]_n$) was used for additional averaging by using the multiple spin-echoes [20,21,33], thereby decreasing the time needed to acquire a fluorine profile. An inter-echo time setting of $2\tau = 150$ μs was used. This resulted in a total acquisition time of approximately 1 day for a single fluorine concentration profile. The amount of averages needed to obtain a hydrogen profile is in the order of 10^3 , and these can be acquired within 10 min. It has to be remarked that fluorine depth profiling of coatings with a low amount of fluorine can only be achieved if the signal relaxation is at least slower than the necessary acquisition time for a single echo ($2\tau = 150$ μs). In general, the higher the polymer mobility, the slower the signal decay (which is indicated by the T_2 -relaxation time) [22,23]. In practice, the T_g of the polymer film should be below room temperature in order to obtain sufficiently strong signal.

2.3. Depth profiling by XPS in combination with microtoming

XPS measurements were performed with a VG-Escalab 200 spectrometer using an aluminum anode (Al $K\alpha = 1486.3$ eV) operating at 510 W with a background pressure of 2×10^{-9} mbar. Spectra were recorded using the VGX900 data system. All carbon 1s (C1s) peaks corresponding to hydrocarbon were calibrated at a binding energy of 285 eV to correct for the energy shift caused by charging. Spectra were acquired at two different take-off angles relative to the surface normal: 0° and 60° , corresponding to the probe depths of ~ 10 and ~ 5 nm, respectively [34]. The fluorine-to-carbon (F/C) ratio was determined from curve fitted C1s window spectra, according to different carbon environment (C–C/C–H; C–O/C–N; C=O; C–F₂; C–F₃ bonds). The F/C ratio was estimated from the corresponding area ratios by:



Scheme 1. Chemical structure of TMP-PCL and Rf_8 -PCL-OH.

$$F/C = \frac{[A(\text{CF}_2) \cdot 2 + A(\text{CF}_3) \cdot 3]}{[A(\text{CF}_3) + A(\text{CF}_2) + A(\text{C}=\text{O}) + A(\text{C}-\text{O}) + A(\text{CC}/\text{CH})]}$$

A special home-made sample holder was used to cut slices of the coating using a Cryostat HM 550 (Microm Systems) instrument. The substrate and sample holders were specially designed to ensure the plane parallelity with the surface when microtoming the film. The cutting was performed at a temperature around the T_g of the coating in order to reduce the roughness introduced by the microtoming knife. The thickness of each slice was approximately 30 μm . XPS spectra were recorded for the top surface of each slice. An estimated error on the real thickness of the slices is about 10%.

3. Results and discussion

3.1. MRI depth profiling

We have recently shown that the fluorine-rich layer in fluorinated PU and epoxy films is very thin (approximately 20 nm) [7,10]. However, to our knowledge, the fluorine profile in a coating beyond the first 100 nm of surface has not been measured so far. To gain insight on the fluorine concentration profile through the whole depth of the film, MRI has been used.

The MRI depth profiling was recorded on a coating (containing 2 wt% of fluorine) cast on a cover glass plate (dimension: $18 \times 18 \times 0.1 \text{ mm}^3$). Coatings were typically 150–200 μm thick. Obtained profiles for hydrogen and fluorine are depicted in Fig. 1. The surface of the coating is located at the left side and the cover glass at the right side of these profiles. The receiver coil is located underneath the glass plate, and signals are acquired from a cylinder of approximately 5 mm in diameter. To obtain high-resolution profile for fluorine, 128 000 repetitions were needed together with 11 echoes from the acquired echo train (containing 256 echoes in total). It is reasonable to consider that the hydrogen concentration is uniform throughout the coating. Therefore, the normalized hydrogen MRI profile can be used as an internal standard for the normalization of the fluorine MRI profile. In

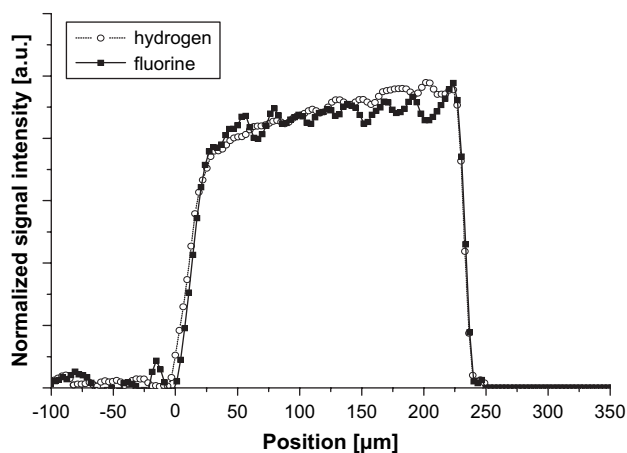


Fig. 1. MRI full-depth profiles of fluorine and hydrogen of a fluorinated PU coating containing 2 wt% F.

Fig. 1, the fluorine and hydrogen profiles, within the experimental error, vary in a similar way. Based on these spectra, we deduced that the fluorine concentration is constant along the full depth of a coating within the spatial resolution of 5 μm . Note that this means that spatial variations in the fluorine content on length scales far below 5 μm will be averaged out and are thus not observed.

The uniform fluorine distribution observed by MRI is surprising at first glance since one would expect that surface segregation of the fluorinated species would yield nonuniform distribution profile at least at the surface [6–10]. However, each MRI data point represents the average F content over a 5 μm section of a coating, and the strong segregation is only present in the first $\sim 20 \text{ nm}$ [10], so the bulk values would level out the surface value for the MRI profiling.

To prove that changes in the fluorine concentration can be determined using the high spatial resolution MRI setup, two samples with different fluorine concentrations (1 and 2 wt% F) were imaged during a single experiment (a glass slide of about 100 μm thick was sandwiched between the coatings [35]), as shown in Fig. 2. The hydrogen profiles were first acquired, followed by the acquisition of the fluorine profiles. For the fluorine profiling 80 000 averages were used, including 11 echoes from the echo train. The lower signal-to-noise ratio, visible at the left side in Fig. 2, was caused by a reduced sensitivity at large distances from the MRI coil and a limited excitation volume. As expected, the hydrogen signal remains at the same level for the two coatings containing different amounts of fluorine. On the other hand, compared to the coating with 2 wt% F, about 40% decrease in the fluorine signal was observed for the coating containing 1 wt% F, indicating that the technique is indeed sensitive enough to detect small fluorine concentration changes in a film. This experiment also demonstrates that MRI can be successfully used for the fluorine depth profiling in multi-layered systems.

We also attempted to check the sensitivity limit for the one-dimensional fluorine profiling by using the current MRI setup. The fluorine profiles of two PU films containing 1 and 0.5 wt%

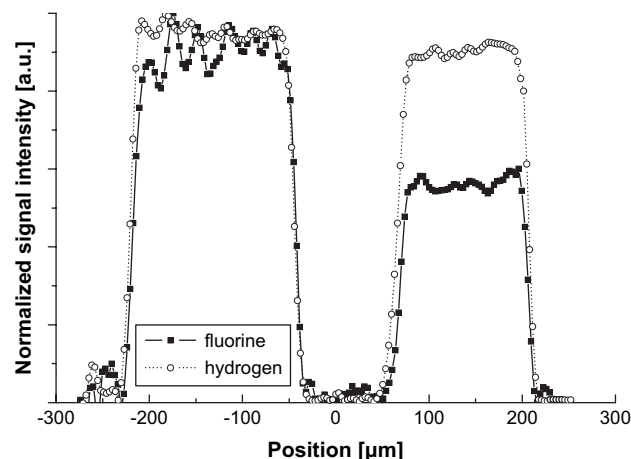


Fig. 2. MRI fluorine and hydrogen profiles of two PU coatings containing 2 and 1 wt% F, respectively, with a glass slide of about 100 μm thick sandwiched in-between.

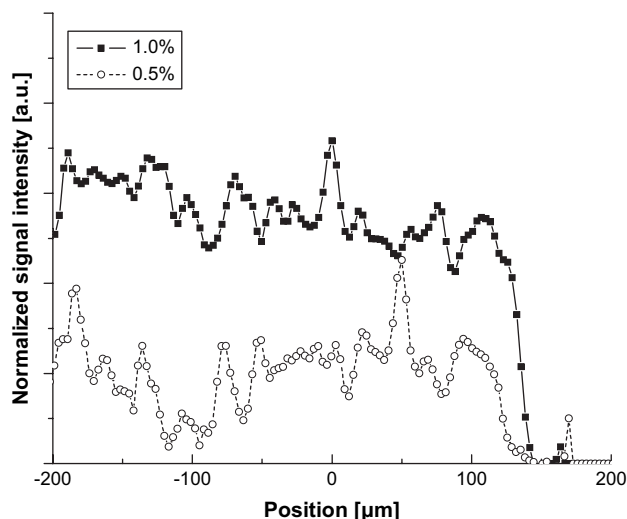


Fig. 3. MRI fluorine profiles of two PU coatings containing 1 and 0.5 wt% F.

F, respectively, are shown in Fig. 3. Obviously, for the film with 0.5 wt% F, the normalized signal intensity is not significantly stronger than the noise level. Therefore, the low sensitivity limit for this MRI setup and the used amount of averages is about 0.5 wt% F.

One may wonder whether this technique can be used for obtaining absolute data on the fluorine concentration. The fluorine concentration at certain depths can be calculated by integrating over the MRI profile (the slope introduced by measurement has to be corrected by dividing the fluorine profile with the hydrogen profile) and coupling that result to the known amount of added fluorine. The absolute values of fluorine concentrations can also be investigated if, prior to the profiling of film with an unknown fluorine concentration, the MRI setup is calibrated with films with a known fluorine content. It should be noted that in this case the fluorine T_2 value for calibration standards and the investigated film should be similar [17].

3.2. Depth profiling by XPS in combination with microtoming

The as-prepared PU film was also subjected to XPS measurements. The results are depicted in Fig. 4; the XPS C1s spectra for two different probe depths (5 and 10 nm) clearly show that the CF_2 peak area decreases significantly within the first few nanometers. This shows that the amount of F-species decreases substantially for fluorinated PU coatings within the first few nanometers.

XPS measurements, in combination with microtoming, were used to check whether the fluorine profile as measured with MRI truly represents the fluorine profile in bulk. The MRI data of the PU coating containing 2 wt% F (Fig. 1) were compared with F/C ratio obtained by XPS in combination with microtoming. For this purpose, the reaction mixture was cast on a special substrate (glass plate glued on the metal carrier). The specimen was then cured at the same reaction

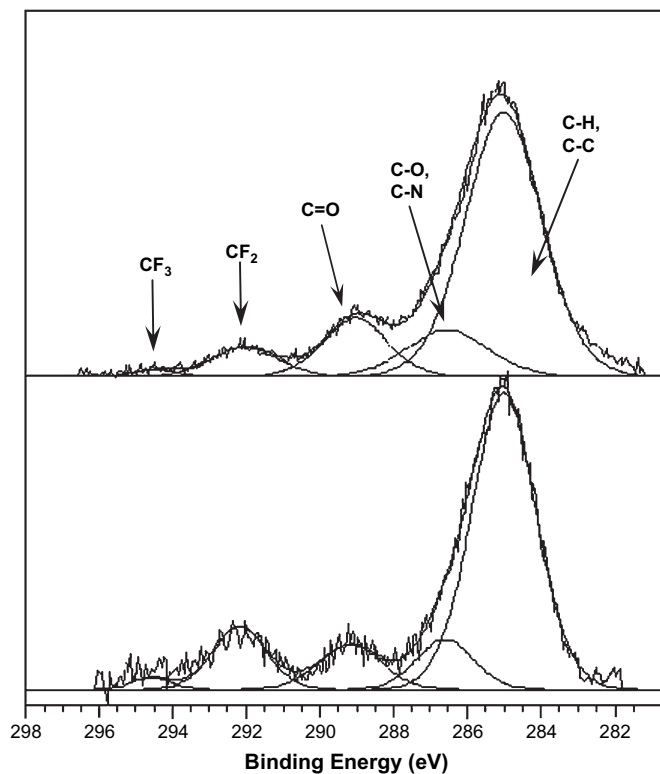


Fig. 4. XPS C1s signals of a fluorinated polyurethane coating containing 2 wt% F. The spectra were recorded at take-off angles of 0° (upper) and 60° (bottom), corresponding to the probe depth of ~ 10 and 5 nm, respectively.

conditions as the PU films containing 2 wt% F previously prepared for MRI measurements. After curing, the coating was sliced into plane-parallel slices using the cryomicrotome. XPS spectra were collected from the top surface of each slice, corresponding to certain depth of the original coating.

Fig. 5 shows F/C ratios recorded on the surface of each slice obtained by microtoming at different depths of the coating. The film depth '0 μm ' represents the virgin surface of the film, while '120 μm ' is very close to the glass substrate slide. The average F/C ratio was over the top 10 nm of the surface of each slice. Note that for the virgin surface the F/C ratio in the

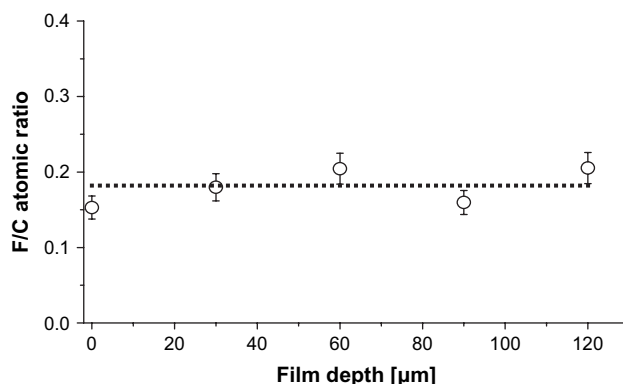


Fig. 5. XPS depth profile of a PU coating containing 2 wt% F. Each point corresponds to F/C ratio at different film depths in the top 10 nm of the surface of each slice. The dashed line is added to merely aid eyes.

top 5 nm is 0.28 (from Fig. 4), significantly greater than the ratio in the top 10 nm which is ~ 0.16 . Within the experimental error of the measurement and the fitting procedure, the F/C ratio is constant along the full depth of the coating. Throughout the coating depth, the F/C ratio obtained by XPS appears to be much higher than one would expect from the bulk F/C ratio from the coating formulation. We speculate that the highly mobile perfluoroalkyl end-capped chains of the coating (due to the PCL spacer with a T_g of -60°C) are able to easily reorient themselves toward the “fresh” surface after it has been created by microtoming, rendering them “visible” by XPS, a technique very sensitive for the depth of first few nanometers of the surface. More investigations on the self-replenishing behavior of such fluorinated tails are under way in our laboratories.

Both MRI and XPS results indicate that the fluorine concentration is constant along the full depth of the PU coatings, with the exception of the top 10 nm. On the other hand, it is difficult to directly compare the XPS results and MRI depth profiling, because the fluorine concentration by XPS is averaged over the top ~ 10 nm of each of the $30\text{-}\mu\text{m}$ slice while the MRI profile is averaged over $5\text{-}\mu\text{m}$ depth in the bulk of the coating. One may consider that these two techniques are complementary for investigating polymeric films in which the chemical composition varies along the film depth. We believe that this MRI technique may be particularly suitable for multi-layer systems, as clearly demonstrated in Fig. 2. We also hope that this proof-of-concept study may serve as a stepping stone to stimulate further investigations on other polymer systems of interests by using the ^{19}F MRI setup.

4. Conclusions

We have demonstrated that fluorine profiles can be obtained along the full depth of fluorinated polyurethane films with a resolution of $5\text{-}\mu\text{m}$ by using high spatial resolution MRI in a nondestructive manner. Fluorine concentrations as low as 0.5 wt% can be detected by this technique. The homogeneous distribution of fluorine in the bulk observed by MRI was consistent with the profile obtained from XPS in combination with microtoming. The MRI setup will also be useful for detecting and quantifying the diffusion of fluorine-containing species between different layers in a multi-layer system.

Acknowledgements

This research forms part of the research program of the Dutch Polymer Institute (DPI), Project #423. We thank Dr. Reinout Hesselink for assistance in microtoming and using the facilities at the Laboratory of Soft Tissue Engineering,

Department of Biomedical Technology, Eindhoven University of Technology.

References

- [1] Hougham G, Cassidy PE, Johns K, Davidson T, editors. Fluoropolymers 1 and 2. New York: Kluwer Academic/Plenum Publishers; 1999.
- [2] Vink P, Bots TL. Prog Org Coat 1996;28:173.
- [3] Walbridge DJ. Prog Org Coat 1996;28:155.
- [4] Anton D. Adv Mater 1998;10:1197.
- [5] Mason R, Jalbert CA, O'Rourke Muisener PAV, Koberstein JT, Elman JF, Long TE, et al. Adv Colloid Interface Sci 2001;94:1.
- [6] Ming W, Laven J, van der Linde R. Macromolecules 2000;33:6886.
- [7] Ming W, Tian M, van de Grampel RD, Melis F, Jia X, Loos J, et al. Macromolecules 2002;35:6920.
- [8] Ming W, Melis F, van de Grampel RD, van Ravenstein L, Tian M, van der Linde R. Prog Org Coat 2003;48:316.
- [9] van Ravenstein L, Ming W, van de Grampel RD, van der Linde R, de With G, Loontjens T, et al. Macromolecules 2004;37:408.
- [10] van de Grampel RD, Ming W, van Gennip WJH, van der Velden F, Laven J, Niemantsverdriet JW, et al. Polymer 2005;46:10531.
- [11] van de Grampel RD, Ming W, Gildenpfnennig A, van Gennip WJH, Laven J, Niemantsverdriet JW, et al. Langmuir 2004;20:6344.
- [12] Game Ph, Sage D, Chapel JP. Macromolecules 2002;35:917.
- [13] Hinder SJ, Watts JF, Lowe C. Surf Interface Anal 2004;36:1032.
- [14] Yokoyama H, Kramer EJ, Rafailovich MH, Sokolov J, Schwarz SA. Macromolecules 1998;31:8826.
- [15] Akamatsu K, Deki S. Scripta Mater 2001;44:2149.
- [16] Hu X, Zhang W, Si M, Gelfer M, Hsiao B, Rafailovich M, et al. Macromolecules 2003;36:823.
- [17] Glover PM, Aptaker P, Bowler C, McDonald PJ. J Magn Reson 1999;139:90.
- [18] Ciampi E, Goerke U, Keddie JL, McDonald PJ. Langmuir 2000;16:1057.
- [19] Chowdhury MA, Hill DJT, Whittaker AK. Biomacromolecules 2004;5:971.
- [20] Gorce JP, Bovey D, McDonald PJ, Palasz P, Taylor D, Keddie JL. Eur Phys J E 2002;8:421.
- [21] Ouriadov AV, MacGregor RP, Balcom BJ. J Magn Reson 2004;169:174.
- [22] Litvinov VM, Dias AA. Macromolecules 2001;34:4051.
- [23] Adriaensens P, Pollaris A, Kelchtermans M, Gelan J. Macromolecules 2003;36:706.
- [24] Erich SJF, van der Ven LGJ, Huinink HP, Pel L, Kopinga K. J Phys Chem B 2006;110:8166.
- [25] Erich SJF, Laven J, Pel L, Huinink HP, Kopinga K. Prog Org Coat 2006;55:105.
- [26] Erich SJF, Laven J, Pel L, Huinink HP, Kopinga K. Appl Phys Lett 2005;86:134105/1.
- [27] Erich SJF, Laven J, Pel L, Huinink HP, Kopinga K. Prog Org Coat 2005;52:210.
- [28] Schwarz R, Schuurmans M, Seelig J, Künnecke B. Magn Reson Med 1999;41:80.
- [29] Murugesan R, English S, Reijnders K, Yamada K, Cook JA, Mitchell JB, et al. Magn Reson Med 2002;48:523.
- [30] Higuchi M, Iwata N, Matsuba Y, Sato K, Sasamoto K, Saido TC. Nature Neurosci 2005;8:527.
- [31] Endo T, Shibasaki Y, Sanda F. J Polym Sci Part A Polym Chem 2002;40:2190.
- [32] Sanda F, Sanada H, Shibasaki Y, Endo T. Macromolecules 2002;35:80.
- [33] Ostroff ED, Waugh JS. Phys Rev Lett 1966;16:1097.
- [34] Tanuma S, Powell CJ, Penn DR. Surf Interface Anal 1994;21:165.
- [35] Perlo J, Casanova F, Blümich B. J Magn Reson 2005;176:64.